

"This document is the Accepted Manuscript version of a Published Work that appeared in final form in Nature Reviews Chemistry, copyright © 2019 Springer Nature Publishing AG. after peer review and technical editing by the publisher. To access the final edited and published work see:

<https://www.nature.com/articles/s41570-019-0096-0#rightslink>

The development of molecular water oxidation catalysts

Roc Matheu,^{a,b} Pablo Garrido-Barros,^{a,b} Marcos Gil-Sepulcre,^a Mehmed Z. Ertem,^c Xavier Sala,^d Carolina Gimbert-Suriñach^a & Antoni Llobet^{a,d,*}

^a Institute of Chemical Research of Catalonia (ICIQ), Barcelona Institute of Science and Technology (BIST), Avinguda Països Catalans 16, 43007 Tarragona, Spain.

^b Departament de Química Física i Inorgànica, Universitat Rovira i Virgili, Marcel·lí Domingo s/n, 43007 Tarragona, Spain.

^c Chemistry Division, Energy & Photon Sciences Directorate, Brookhaven National Laboratory, Upton, New York, 11973-5000, USA.

^d Departament de Química, Universitat Autònoma de Barcelona, Cerdanyola del Vallès, 08193 Barcelona, Spain.

Email: allobet@iciq.cat

Abstract | There is an urgent need to transition from fossil fuels to solar fuels — not only to lower CO₂ emissions that cause global warming, but also to ration fossil resources. Splitting H₂O with sunlight emerges as a clean and sustainable energy conversion scheme that can afford practical technologies in the short to midterm. A crucial component in such a device is a water oxidation catalyst (WOC). These artificial catalysts have mainly been developed over the last two decades, which is in contrast to Nature's WOCs, which have featured in its photosynthetic apparatus for more than a billion years. This time period has seen the development of increasingly active molecular WOCs, the study of which affords an understanding of catalytic mechanisms and decomposition pathways. This Perspective offers a historical description of the landmark molecular WOCs, particularly ruthenium systems, that have guided research to our present degree of understanding.

Graphical abstract

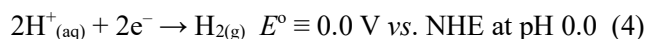
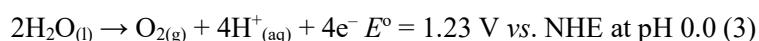
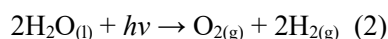
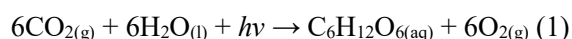
Table of contents blurb

Water oxidation catalysts are key components in water-splitting devices for sustainable schemes to synthesize fuels by using energy, including that from sunlight. This Perspective presents historical developments in the molecular water oxidation catalysis field, placing particular emphasis on studies of ruthenium complexes that have taught us much about how to design optimal catalysts.

[H1] Introduction

Global warming of our planet threatens the wellbeing of modern societies as we know them.^{1,2,3,4} This threat has brought together environmentally educated scientists and laypersons to urge world leaders and politicians to develop policies that ensure the long-term preservation of our planet while maintaining our societal lifestyle.^{5,6} Among the most promising of these policies are those based on a circular economy and low carbon emissions. The concept of a circular economy relies on green chemistry and catalysis, and thus highlights the key role chemistry plays in society today as well as the important role it will likely play in solving problems in the near future.⁷ The main contributors to global warming are fossil fuels, the use of which generates 80–85% of all the anthropogenic energy used on Earth.^{8,9} This warming, as well as the non-renewable nature of these fuels, see it imperative to develop sustainable and clean energy conversion schemes.

Nature has been using photosynthesis for a billion years^{10,11,12} to generate carbohydrates from CO₂ and H₂O (eq. 1), storing solar energy in chemical bonds by driving a thermodynamically uphill conversion. Splitting H₂O with sunlight (eq. 2) can be regarded as an analogous reaction to photosynthesis^{13,14,15,16,17} in that both reactions are thermodynamically uphill and driven by sunlight. Moreover, in both cases the use of sunlight to drive the reaction requires intermediate molecules (or materials) capable of transferring the sunlight energy to activate catalysts. Lastly, both conversions are redox reactions in which the oxidation half-reaction is the conversion of H₂O to O₂ (eq. 3). The reactions only differ in their reductions: in photosynthesis, CO₂ is reduced to hydrocarbons, while in water splitting H⁺ is reduced to H₂ (eq. 4).



The slow kinetics of the H₂O oxidation reaction calls for catalysis, which, if economically viable, could see sunlight-driven H₂O splitting (WS-*hν*) as a potential solution to today's energy problem. Concomitantly, the H₂ evolved at the cathode could be used later to react with O₂ to generate H₂O and release energy. Alternatively, the H₂ can be used to hydrogenate CO₂ to give CO, MeOH, CH₄ or synthetic hydrocarbons using the Fischer–Tropsch process.^{18,19,20} These energy vectors, if obtained in this way, are referred to as solar fuels and could form the basis for an energy democracy within a circular economy.²¹

Performing $WS-h\nu$ in an efficient manner requires access to an active and robust water oxidation catalyst (WOC). This role is filled in Nature by the oxygen evolving complex in photosystem II (OEC-PSII), which features a Mn_4Ca cubane cluster (FIG. 1a).^{22,23,24,25} The OEC-PSII converts two H_2O molecules into O_2 on the millisecond time scale (1.6 ms) by a series of sunlight-induced charge transfer steps known as the Kok cycle.^{26,27,28,29,30} The Mn_4Ca cluster is reassembled approximately every 10–15 minutes due to the damage induced on the amino acid residues coordinated to the cluster, as a result of reacting with photogenerated 1O_2 .^{31,32} Given the lifetime of the cluster and the rate at which it evolves O_2 , we can estimate that its turnover number (TON) is on the order of 10^6 .

Figure 1 | Nature uses metalloenzymes to effect redox reactions that consume or afford H_2O . **a** | The oxygen-evolving complex in photosystem II is a Mn_4Ca cluster that mediates the Kok cycle, in which light energy input enables the oxidation of $2H_2O$ to O_2 . A proposed structure of the cluster from the protein in its S_0 state is drawn. **b** | The active site of cytochrome P450 enzymes activates O_2 to give H_2O and the oxo complex $[Fe(\text{porphyrinato})(\text{cysteinato})(O)]$, which goes on to oxidize organic substrates. An X-ray structure of the oxo complex is presented. Part **a** is adapted with permission from [REF. 30](#), Elsevier. Part **b** is adapted with permission from [REF. 79](#).

One of the key features of the OEC-PSII is its capacity to carry out a series of consecutive redox reactions at potentials close to the thermodynamic value of the $2H_2O_{(l)} \rightarrow O_{2(g)} + 4H^+_{(aq)} + 4e^-$ half-reaction. Indeed, one can imagine that sequential oxidations should become more difficult, but not if the phenomenon of redox leveling is at play. This is enabled by proton-coupled electron-transfer (PCET) processes^{33,34,35,36} that see the initial resting state S_0 undergoing four light-driven oxidations to give S_4 , the state that can release O_2 . Three of these steps involve the simultaneous removal of H^+ and e^- or a single H atom. In this way, the Mn_4Ca cluster sees its Mn centres undergo sequential oxidations, which in three cases do not change the overall charge of the cluster until the generation of O_2 .³⁷ Thus, the cluster is progressively activated until it reaches a state that is sufficiently reactive to generate an O–O bond. The exact molecular details of how this occurs remains a topic of debate.^{38,39,40,41} For contrast, Nature can not only convert H_2O to O_2 but can also reduce O_2 back to H_2O with concomitant oxidation of an organic substrate, as occurs in cytochrome (Cyt) P450 enzymes (FIG. 1b).

Synthetic WOCs can be broadly classified into two main groups: oxides^{42,43,44} and molecular complexes.^{45,46,47} The use of oxides as H_2O oxidation catalysts can be traced back to 1903 and a

report by Cohen and Gläser about their attempted measurement of the potential of a Co^{III/II} couple, which resulted instead in the deposition of CoO_x on their electrode and large currents that reflect catalytic H₂O oxidation.⁴⁸ In contrast, the first well-defined molecular WOC came in 1982, and this so-called ‘blue dimer’ (**1**, FIG. 2) was reported at a time when coordination chemistry was already well established.⁴⁹ Since then, a large number of complexes capable of oxidizing H₂O to O₂ have emerged, prominent examples of which are presented in FIG. 2. This Perspective presents a historical account of molecular WOCs and places emphasis on systems that, at the time they were reported, advanced our understanding of the field.

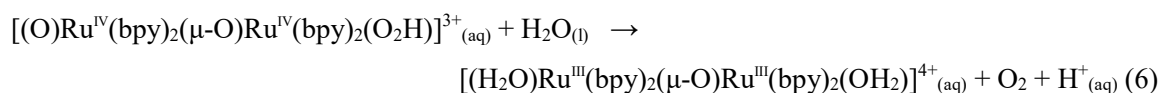
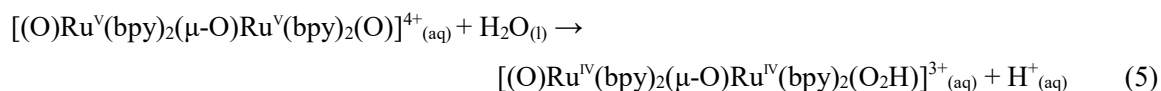
Figure 2 | Transition metal complexes of N-donor ligands are prominent H₂O oxidation catalysts. bbp⁻, (3,5-bis(2,2'-bipyridin-6-yl)pyrazolate); bda²⁻, 2,2'-bipyridine-6,6'-dicarboxylate; bpm, 2,2'-bipyrimidine; bpp⁻, 3,5-bis(2-pyridyl)pyrazolate; bpy, 2,2'-bipyridine; misoq, 6-methoxyisoquinoline; mox⁴⁺, N¹,N^{1'}-(1,2-phenylene)bis(N²-methyloxalamide); ppy⁻, 2-(2-phenylido)pyridine; py, pyridine; tda²⁻, 2,2':6',2''-terpyridine-6,6''-dicarboxylate; tpm, tris(2-pyridyl)methane; tpy, 2,2':6',2''-terpyridine.

[H1] The blue dimer and the early days

It was long ago observed that simply adding [(bpy)₃Ru^{III}]³⁺ (bpy = 2,2'-bipyridine) to H₂O resulted in the evolution of O₂. However, neither the mechanism nor the potential high oxidation states and active species for the O–O bond formation were characterized.^{50,51} Thus, shortly thereafter, the report on the blue dimer saw it become the first well-characterized molecular complex that behaves as a H₂O oxidation catalyst in the presence of a sacrificial oxidant. The ‘blue dimer’ *cis*-[(H₂O)Ru^{III}(bpy)₂(μ-O)Ru^{III}(bpy)₂(OH₂)]⁴⁺ is a complex wherein two Ru^{III} centres are bridged by an oxo group to give a complex with a strong absorption at λ_{max} = 637 nm (ε = 21100 M⁻¹cm⁻¹ at pH 1.0).⁵² The pseudo-octahedral Ru^{III} sites each feature two bpy co-ligands in a *cis* arrangement with the last position being occupied by an aquo group. The redox properties of this complex have been thoroughly studied by electrochemistry, which shows that the higher Ru oxidation states required for catalysts are indeed accessible.⁵² In **1** and other Ru complexes described here, at the potentials relevant to H₂O oxidation it is usually the Ru centres and/or the oxygenic ligands that undergo redox rather than the co-ligands.

At pH 1.0, where most of the catalytic H₂O oxidation reactions have been carried out for **1**, the blue dimer undergoes two redox processes. First, the [(H₂O)Ru^{III}(bpy)₂(μ-O)Ru^{III}(bpy)₂(OH₂)]⁴⁺ species undergoes loss of H⁺ and e⁻ at E^o = 0.79 V (all redox potentials here are reported against the normal

hydrogen electrode, NHE) to give $[(\text{H}_2\text{O})\text{Ru}^{\text{III}}(\text{bpy})_2(\mu\text{-O})\text{Ru}^{\text{IV}}(\text{bpy})_2(\text{OH})]^{4+}$. In order to easily keep track of electron counts, we denote formal oxidation states in this Perspective; for Ru in oxidation states above +III, electron density is removed both from the Ru centre and any O^{2-} ligand bonded to it, conferring oxyl character (O^-) on the ligand. Second, further oxidation involves loss of 3e^- and 3H^+ in a single step at $E^\circ = 1.22\text{ V}$ to afford $[(\text{O})\text{Ru}^{\text{V}}(\text{bpy})_2(\mu\text{-O})\text{Ru}^{\text{V}}(\text{bpy})_2(\text{O})]^{4+}$. Taken together, these two processes result in the removal of the 4H^+ and 4e^- required for the oxidation of $2\text{H}_2\text{O}$ molecules to O_2 (eq. 3), as occurs in the OEC-PSII. It was initially thought that $[(\text{O})\text{Ru}^{\text{V}}(\text{bpy})_2(\mu\text{-O})\text{Ru}^{\text{V}}(\text{bpy})_2(\text{O})]^{4+}$ would undergo intramolecular coupling of the two $\text{Ru}^{\text{V}}=\text{O}$ units to liberate O_2 and give back, on aquation, the starting complex $[(\text{H}_2\text{O})\text{Ru}^{\text{III}}(\text{bpy})_2(\mu\text{-O})\text{Ru}^{\text{III}}(\text{bpy})_2(\text{OH}_2)]^{4+}$.⁵³ This mechanism involves the interaction of two M–O units (I2M) but is now thought not to be operative here. Instead, kinetics and labeling experiments showed that O–O bond formation occurs through water nucleophilic attack (WNA) on a $\text{Ru}^{\text{V}}=\text{O}$ unit to form a $\text{Ru}-\text{O}_2\text{H}$ intermediate prior to O_2 liberation (eq. 5,6).⁵³ Despite this conclusion, isotopic labeling experiments performed under the exact same conditions led to contradictory results, reflecting the difficulty of carrying out such experiments, in which headspace contamination with atmospheric O_2 can easily take place.^{54,55,56,57}



In the presence of excess Ce^{IV} , a sacrificial 1e^- oxidant,⁵⁸ **1** oxidizes H_2O to O_2 with 4–5 turnovers and an initial turnover frequency (TOF; FIG. 3) of $4.2 \times 10^{-3}\text{ s}^{-1}$.⁵² It is assumed that one of the major shortcomings for this catalyst is the coordination of anions (anation), a process that competes with aquation and deactivates the system.^{59,60} The TOF of a catalyst is highly sensitive to the conditions under which it is studied, although Figure 3 affords a reasonable qualitative picture of catalyst evolution because all the TOF values were determined at pH 1.0 (except for that of **11**, which was determined at pH 10.0).

The TOF values can be measured chemically using a sacrificial electron acceptor reagent, as is the case just described for **1**, but can also be measured electrochemically that is by applying a potential through an electrode. In the chemical case the potential generated is limited by the redox potential of the sacrificial reagent whereas in the electrochemical case the applied potential can be varied basically at will. In the electrochemical case the Foot of the Wave Analysis (FOWA) developed by

Saveant et al.,⁶¹ has become one of most convenient ways to calculate TOF. Since the TOF values are dependent on the applied potential, FOWA generally reports the maximum achievable value for a given catalyst, that is named TOF_{max}.

What becomes clear is that for more than 20 years the blue dimer **1** and related derivatives^{62,63} were the only well-characterized molecular WOCs. One of the main challenges to developing new Ru catalysts was the unavailability of rational synthetic strategies for the preparation of dinuclear oxo-bridged aquo complexes. A breakthrough came with the realization that the O²⁻ bridge was not indispensable for WOC activity. Thus, it became possible to use alternative bridging ligands, particularly organic N-donors as in [(H₂O)Ru^{II}(tpy)(μ-bpp)Ru^{II}(tpy)(OH₂)]³⁺ (**2**, tpy = 2,2':6',2''-terpyridine, bpp⁻ = 3,5-bis(2-pyridyl)pyrazolate), where a pyrazolate moiety in bpp⁻ bridges the two Ru centres⁶⁴. Complex **2** is notable in that its two Ru–OH₂ groups are rigidly held in an orientation in which the O atoms are very close together and thus ready to undergo intramolecular coupling once **2** is suitably oxidized. Indeed, oxygen labeling experiments and theoretical calculations confirmed that this process can occur, and this system is the first synthetic example in which an O–O bond is generated through an I2M mechanism.^{65,66,67} This preorganization of the active Ru–O groups greatly favours the reaction by minimizing any activation entropy and leading to a TOF of 1.4 × 10⁻² s⁻¹ — 3.4 times greater than that of the blue dimer **1**.

Figure 3 | **The evolution of molecular H₂O oxidation catalysts.** Refined designs enable the turnover frequency (TOF) for the conversion of 2H₂O to O₂ to even exceed that of the oxygen-evolving complex in photosystem II (OEC-PSII). TOF values for complexes were determined at pH 1.0 chemically using Ce(IV) as sacrificial oxidant, except in the case of **11**, when pH 10.0 electrolyte was used and the TOF was determined electrochemically.

Being able to use organic bridging ligands enabled synthetic chemists to rapidly develop new Ru WOCs. This synthetic strategy of avoiding O²⁻-bridged species has since afforded a family of diruthenium complexes in which auxiliary ligands can control the mechanistic pathway through which O–O bond formation occurs. This is nicely illustrated in the case of [(H₂O)Ru^{II}(tpm)(μ-bpp)Ru^{II}(tpm)(OH₂)]³⁺ (**3**, tpm = tris(2-pyridyl)methane), a derivative of **2** in which the meridional tpy ligand has been substituted with the facial tpm ligand. With this new structural arrangement, the two aquo groups that were facing one another in **2** are now situated *trans* to each other in **3**. As a result, the intramolecular I2M pathway is not accessible for **3** and O–O bond formation instead proceeds through an intermolecular I2M pathway. Moving from the tetradentate ligand bpp⁻ to the

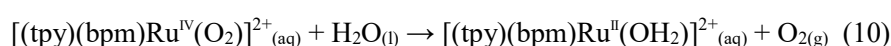
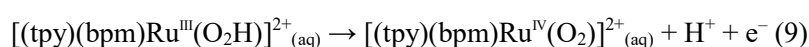
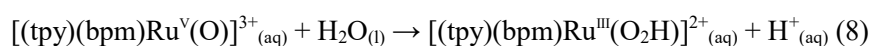
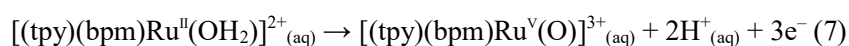
hexadentate ligand bbp^- (3,5-bis(2,2'-bipyridin-6-yl)pyrazolate) affords yet another distinct motif. In $[(\text{H}_2\text{O})\text{Ru}^{\text{II}}(\text{py})_2(\mu\text{-bbp})\text{Ru}^{\text{II}}(\text{py})_2(\text{OH}_2)]^{3+}$ (**4**, py = pyridine),⁶⁸ for example, the equatorial bbp^- ligand constrains the bond angles at the Ru centres in the equatorial plane, thereby separating the two Ru–OH₂ moieties in **4** relative to those in **2**. Thus, **4** cannot participate in an I2M pathway but instead undergoes the O–O bond formation through a WNA path.

Although isotopic labeling experiments and measurements of the relative abundance of evolved O₂ isotopologues afforded contradictory results in the case of **1** (probably due to leakage of atmospheric O₂), the labeling experiments provided very consistent data for **2–4**. This is important because these experiments provide extremely valuable mechanistic information that allows the unambiguous identification of the O–O bond formation pathway. The high quality of the data obtained for **2–4** is partly due to today's commercially available mass spectrometry instrumentation, which allow one to interface atmospheric pressure reaction vessels directly to a high vacuum measurement chamber.

[H1] The 'one site is enough' revolution

Although the emergence of dinucleating organic ligands does enable the synthesis of many complexes, preparing tailored dinuclear Ru–OH₂ complexes remains a difficult task that can take years of synthetic efforts.⁶⁹ In comparison, a targeted mononuclear Ru–OH₂ complex can typically be prepared in weeks, making it very desirable to see if one could develop active mononuclear WOCs. Indeed, when the mononuclear complex $[(\text{ntp})(\text{mpy})_2\text{Ru}^{\text{II}}(\text{OH}_2)]^{2+}$ (**5**, mpy = 4-methylpyridine, ntp = 2,6-di(1,8-naphthyridin-2-yl)-4-*tert*-butyl-pyridine) was reported⁷⁰ to behave as a H₂O oxidation catalyst, a revolution in the field ensued because easy access to Ru WOCs was conceivable. Indeed, many research efforts were directed at studying mononuclear Ru complexes as WOC candidates, affording a better understanding of WOC mechanisms in general. This knowledge contributed to the development of faster catalysts that emerged from 2005 onwards (FIG. 3). Methodology also became more reliable, although the paper describing the catalytic activity of **5** included a mass balance violation.⁷⁰ The maximum amount of O₂ that can be produced under the conditions reported assuming 100% chemical efficiency would give a TON of 228, less than half of the reported TON of 580. This error, which was corrected in a subsequent publication, is most likely due to miscalibration of the polarographic probe used to quantify the generated O₂ gas. We stress again that the execution of catalytic experiments in this field requires utmost care.

In 2005, the activity of mononuclear complexes was puzzling because it was assumed that a dinuclear-diaquo complex (or larger system) was needed to be able to remove 2H^+ and 2e^- from each Ru–OH₂ group. This mystery was solved a few years later when the mechanistic analysis of $[(\text{tpy})(\text{bpm})\text{Ru}^{\text{II}}(\text{OH}_2)]^{2+}$ (**6**, bpm = 2,2'-bipyrimidine) showed that one Ru site was enough to carry out H₂O oxidation catalysis.⁷¹ It was proposed that the initial Ru^{II}–OH₂ complex undergoes a series of e⁻/H⁺ transfers to give the active species Ru^V=O (eq. 7).



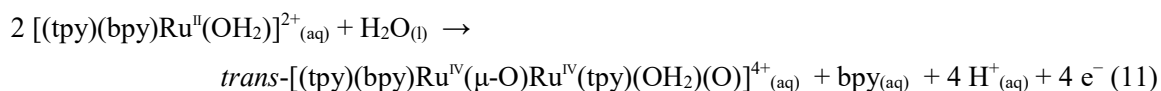
A similar reasoning is also proposed for the related complex $[(\text{tpy})(\text{bpy})\text{Ru}^{\text{II}}(\text{OH}_2)]^{2+}$, and this mechanism is consistent with its Pourbaix diagram (FIG. 4a), which, as will become clear indicates that it is less electron-rich than $[(\text{bda}-\kappa\text{-N}^2\text{O})(\text{py})_2\text{Ru}^{\text{II}}(\text{OH}_2)]$ (**9**(OH₂)), which features an anionic ligand (FIG. 4b).^{72,73,74,75} In any case, once the Ru^V=O species is generated, kinetics experiments support a WNA mechanism that gives the corresponding hydroperoxo Ru^{III}–O₂H (eq. 8).

Figure 4 | Pourbaix diagrams for Ru complexes indicate stability across a wide pH range. The schemes can be considered phase diagrams of complexes with the variables being potential (E , in V) and pH. **a** | The Pourbaix diagram for $[(\text{tpy})(\text{bpy})\text{Ru}^{\text{II}}(\text{H}_2\text{O})]^{2+}$. **b** | The Pourbaix diagram for $[(\text{bda}-\kappa\text{-N}^2\text{O})(\text{py})_2\text{Ru}^{\text{II}}(\text{OH}_2)]$ (**9**(OH₂)). Blue lines correspond to the Ru^{V/IV} couples, dashed green lines to the standard potential $E^\circ(\text{H}_2\text{O}/\text{O}_2)$ and vertical lines to pK_as. The co-ligands and overall charges are omitted for clarity. bda²⁻, 2,2'-bipyridine-6,6'-dicarboxylate; bpy, 2,2'-bipyridine; py, pyridine; tpy, 2,2':6',2''-terpyridine.

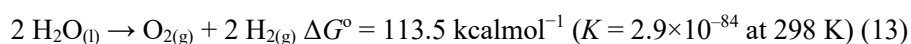
The Ru^{III}–O₂H species undergoes one more oxidative process before liberating O₂ and regenerating the initial Ru^{II}–OH₂ complex (eqs 9,10) to close the catalytic cycle (FIG. 5a). Although a distinct mechanism is possible in another system (FIG. 5b is described below), the present cycle and variations thereof have now been widely proposed for a variety of mononuclear Ru complexes and other mononuclear transition metal complexes proposed to be molecular WOCs.⁷⁶ The mechanism resembles the one by which Cyt-P450 activates O₂ and oxidizes organic substrates (FIG. 1b), although the two processes occur in opposite directions.^{77,78,79}

Figure 5 | **Two mechanisms of molecular H₂O oxidation catalysts. a** | The water nucleophilic attack (WNA) mechanism involves O–O bond formation between an oxo and H₂O substrate. This mechanism is operative for many monoruthenium complexes such as [(tpy)(bpm)Ru^{II}(OH₂)]²⁺ (**6**).⁷¹
b | Alternatively, O–O bond formation can occur through interaction of two M–O units (I2M), a mechanism at play for [(bda)(py)₂Ru] complexes similar to **9**.⁹⁸ bda²⁻, 2,2'-bipyridine-6,6'-dicarboxylate; bpm, 2,2'-bipyrimidine; py, pyridine; tpy, 2,2':6',2''-terpyridine.

The discoveries of the mononuclear catalysts were real breakthroughs because of their ease of preparation and synthetic versatility. However, mononuclear Ru–OH₂ complexes have the propensity to form O²⁻-bridged dinuclear and even polynuclear complexes^{80,81,82} through processes that may compete with H₂O oxidation catalysis. Indeed, the terminal Ru=O/Ru–O⁻ can bridge to another Ru centre instead of undergoing WNA or I2M. The formation of a bridged complex can spell deactivation of the catalyst but can also afford species that are active WOCs, as is the case for [(tpy)(bpy)Ru^{II}(OH₂)]²⁺ (eq. 11).⁸³ In this case, the resulting O²⁻-bridged complex *trans*-[(tpy)(bpy)Ru^{IV}(μ-O)Ru^{IV}(tpy)(OH₂)(O)]⁴⁺ (**7**) is actually a more active and robust catalyst than the parent complex.



The increase in popularity of catalytic H₂O oxidation has afforded a growing family of catalyst candidates featuring Ru or other transition metals. Although we mentioned above that the complexes described here have ligands that are resistant towards oxidation, some other ligands, including those with benzylic/picolinic methylene groups, readily undergo oxidation. Careful analyses of the respective Ru complexes clearly reveals ligand oxidation, in many cases all the way to CO₂.^{84,85,86} To illustrate just how important it is to consider the possibility of oxidation, we now consider the thermodynamics of PhCH₂Me oxidation by H₂O to afford acetophenone and H₂⁸⁷ (eq. 12), analogous to the H₂O splitting reaction (eq. 13).



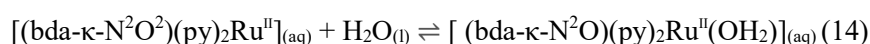
The equilibrium constant of the organic oxidation is more than 67 orders of magnitude larger than that of H₂O splitting (eq. 12,13). Moreover, the kinetics of PhCH₂Me oxidation are also favorable,

as is the case for benzylic/picolinic methylene groups. We thus surmise that there is no way that an initial complex featuring benzylic/picolinic methylene groups can be a true WOC; activity observed when using such a complex likely instead arises from a complex of oxidized ligand(s) or the corresponding oxide cluster.⁸⁸ We express an additional cautionary note with respect to dynamic light scattering (DLS), the detection limit (1–2 nm) of which is greater than the size of low molecular weight clusters, including those derived from Co phosphates.^{89,90} The existence of these oxide clusters can thus not be ruled out using DLS, leading to a typical misinterpretation of data, particularly for first row transition metal complexes. Examples of these complexes can be labile, such that their catalytic activity, which often is attributed to the complex itself, arises instead from metal oxide nanoparticles.^{48,88,91,92}

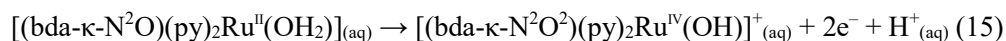
In parallel with research into mononuclear Ru WOCs, a number of Ir complexes have also been developed to serve as WOCs. The first of these was [(ppy)₂Ir^{III}(OH₂)₂]⁺ (ppy⁻ = 2-(2-phenylidene)pyridine) — the first organometallic complex to be used as a WOC. This complex was followed by [(C₅Me₅)(ppy)Ir^{III}Cl] (**8**),⁹³ but later studies showed that **8** readily loses its C₅Me₅⁻ ligand to form Ir–O–Ir complexes.⁹⁴ In retrospect, it is not surprising that a π-acidic ligand such as C₅Me₅⁻ is not able to stabilize Ir in the high oxidation states required for H₂O oxidation. In addition, it was later shown that the putative Ir–O₂H intermediate could undergo an entropically favored intramolecular reaction with the C–H and C–Me bonds of C₅Me₅⁻ to eventually form HCO₂H and MeCO₂H as decomposition products.^{95,96}

[H1] Seven-coordinate complexes and FAME ligands

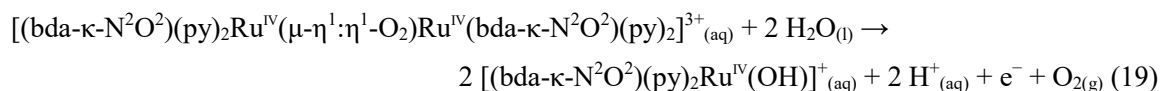
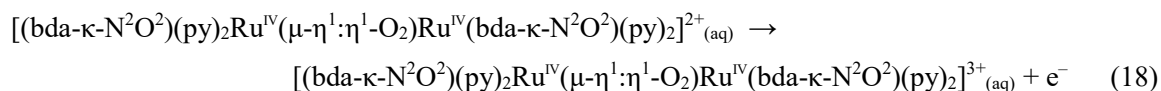
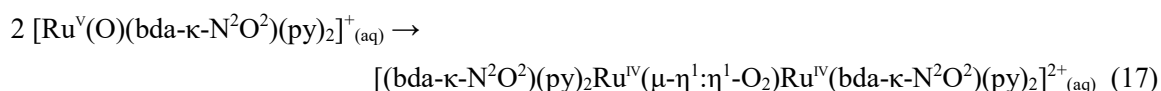
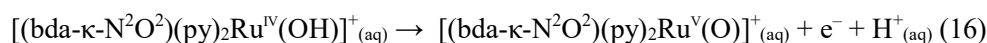
The report of the complex [(bda)(py)₂Ru^{II}] (**9**, bda²⁻ = 2,2'-bipyridine-6,6'-dicarboxylate)^{97,98} represents a turning point for the H₂O oxidation catalysis field. As mentioned in the previous section, preparing mononuclear Ru–OH₂ complexes is relatively easy but still poses some challenges because they must incorporate a substitutionally labile OH₂ ligand. Thankfully, the H₂O adduct of **9** forms on dissolving **9** in H₂O, with the aquo ligand bonding to Ru^{II} at the expense of one of the hemilabile carboxylates (eq. 14).⁹⁹ The system is dynamic at room temperature, and the two carboxylates can coordinate and decoordinate very quickly in order to protect or vacate coordination sites at Ru.¹⁰⁰



The fact that one can generate the Ru–OH₂ complex in situ enormously simplifies the development of a catalyst/precatalyst. Oxidizing the aquo complex in aqueous solution affords a Ru^{IV} species in which the demands of the electrophilic metal not only see it coordinate the py ligands and substrate, but also all four donors in bda²⁻. The seven coordinate centre adopts a pseudo pentagonal bipyramidal geometry in which the axial positions are occupied by the py ligands (eq. 15).



The anionic carboxylate groups in $[(\text{bda-}\kappa\text{-N}^2\text{O}^2)(\text{py})_2\text{Ru}^{\text{IV}}(\text{OH})]^+$ bind the Ru strongly and further electron density comes from the basic OH⁻ group, enabling the stabilization of high oxidation states — Ru^{IV} and Ru^V — just when it is most needed. Indeed, the above phenomena enable **9** to mediate H₂O oxidation catalysis at pH 1.0 at an overpotential of only 170 mV. The strong effects of electron donation and anionic charge on the carboxylates become evident by noting that the redox potential of the Ru^{V/IV} couple for **9**(OH₂) is 800 mV lower than that of $[(\text{tpy})(\text{bpy})\text{Ru}^{\text{II}}(\text{OH}_2)]^{2+}$ (FIG. 4b), a complex that contains only charge-neutral ligands. Indeed, a correlation between the potential of the Ru^{V/IV} couple and the anionic nature of the ligands bonded to Ru has been established that facilitates understanding the effect of ligands on redox potentials.¹⁰¹ On reaching the oxidized Ru^V=O/Ru^{IV}-O state (eq. 16), the complex dimerizes to give the corresponding peroxy intermediate $[(\text{bda-}\kappa\text{-N}^2\text{O}^2)(\text{py})_2\text{Ru}^{\text{IV}}(\mu\text{-}\eta^1\text{:}\eta^1\text{-O}_2)\text{Ru}^{\text{IV}}(\text{bda-}\kappa\text{-N}^2\text{O}^2)(\text{py})_2]^{2+}$ (eq. 17). This dimer, in the presence of excess oxidant, is transformed to the corresponding superoxo that can liberate O₂ (eq. 19, FIG. 5b).



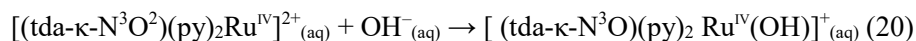
Kinetics experiments conducted at low catalyst concentrations indicate that the dimerization process is the rate-determining step (RDS) of the catalytic cycle. Replacing the axial py ligands in **9** with π -

extended ligands such as 6-methoxyisoquinoline (misoq) affords $[(\text{bda})(\text{misoq})_2\text{Ru}^{\text{II}}]$ (**10**), a WOC with a TOF more than two orders of magnitude greater than that for **9** measured under exactly the same conditions.^{102,103,104,105} The misoq ligands allow for stronger van der Waals and π - π interactions between the $\text{Ru}^{\text{V}}=\text{O}/\text{Ru}^{\text{IV}}-\text{O}^\cdot$ complexes, thereby lowering the activation free energy barrier of the RDS for **10** relative to that for the py derivative **9**. The facile formation of the peroxo dimer $\mathbf{10}(\mu\text{-}\eta^1:\eta^1\text{-O}_2)\mathbf{10}$ (FIG. 2) enables TOFs of around 1000 s^{-1} , which are on the same order of magnitude of those for OEC-PSII (TOF = $1/(1.6\text{ ms}) \approx 600\text{ s}^{-1}$).

We wish to caution the reader against assuming that any Ru complex of N- and O-donor ligands, when dissolved in H_2O and/or treated with an oxidant, will spontaneously afford the requisite Ru-OH₂, Ru-OH or Ru=O group and go on to behave as a WOC. Although this does occur in the case of **9**, it is by no means general. Therefore, thorough characterization of complex intermediates remains indispensable to understanding the chemistry of a particular catalyst candidate. For example, by making invalid assumptions one is at a high risk of reporting inaccurate mechanisms, as transpired in the case of $[(\text{qpy})(\text{py})_2\text{Ru}^{\text{II}}]$ (qpy = 2,2':6',2'':6'',2''':6''',2''''-quaterpyridine), which also features a tetradentate ligand.¹⁰⁶ The addition of Ce(IV) to an acidic solution of $[(\text{qpy})(\text{py})_2\text{Ru}^{\text{II}}]$ generates a large amount of O₂. However, after characterizing the species present in solution after catalysis, it was found that the terminal pyridyl groups of qpy underwent oxidation to afford the corresponding oxide 2,2':6',2'':6'',2''':6''',2''''-quaterpyridine-1,1''''-dioxide (qpy-O₂), which remained bound to Ru. Thus, it appears that $[(\text{qpy-O}_2)(\text{py})_2\text{Ru}^{\text{II}}]$ is the real catalyst,¹⁰⁷ although we still lack clear characterization of the Ru-OH₂/Ru-OH/Ru=O active species. This oxidation of the terminal pyridyl groups does not take place in related complexes such as $[(\text{tpy})(\text{bpy})\text{Ru}^{\text{II}}(\text{OH}_2)]^{2+}$. This has been rationalized in terms of the coordination geometry of qpy, which can only bind four equatorial sites if large distortions from the ideal octahedral Ru geometry are conceded. Thus, strain can be relieved if the terminal pyridyls in qpy undergo decoordination and subsequent intramolecular oxidation by a Ru=O group.

At the time of writing, the best molecular WOC, as judged from TOFs, is $[(\text{tda})(\text{py})_2\text{Ru}^{\text{II}}]$ (tda^{2-} = 2,2':6',2'':6''-terpyridine-6,6''-dicarboxylate).^{108,109} The tda^{2-} ligand contains one more pyridyl group than bda^{2-} but still binds in a tetradentate manner in the complex $[(\text{tda-}\kappa\text{-N}^3\text{O})(\text{py})_2\text{Ru}^{\text{II}}]$ because of the electronic and steric requirements of Ru^{II}. On $2e^-$ oxidation, the Ru^{IV} site binds the previously dangling carboxylate to give the heptacoordinate species $[(\text{tda-}\kappa\text{-N}^3\text{O}^2)(\text{py})_2\text{Ru}^{\text{IV}}]$, which gives rise to a well-resolved ¹H NMR spectrum consistent with it being diamagnetic. At pH 7.0 and higher pHs, the Ru^{IV} centre undergoes OH⁻ substitution of one carboxylate group to generate the

catalytically active species $[(\text{tda-}\kappa\text{-N}^3\text{O})(\text{py})_2\text{Ru}^{\text{IV}}(\text{OH})]^+$ (**11**), which now features a dangling carboxylate (FIG. 2, eq. 20).



Complex **11** enjoys all the benefits associated with the bda^{2-} ligand in **9**: strongly σ -donating anionic carboxylates, a constrained geometry in the equatorial plane and accessible heptacoordinate species at high Ru oxidation states.¹¹⁰ Moreover, **11** has a key additional feature in the form of a decoordinated carboxylate, which is situated so that it can intramolecularly accept H^+ during the O–O bond formation step ($\text{Ru}^{\text{V}}=\text{O} + \text{H}_2\text{O} \rightarrow \text{Ru}^{\text{III}}-\text{O}_2\text{H} + \text{H}^+$, FIG. 6a), as shown using density functional theory calculations.^{108,111} This arrangement favors the WNA over the I2M mechanism by strongly lowering the activation free energy barrier of the WNA RDS, allowing for fast catalysis; a $\text{TOF}_{\text{max}} \sim 8,000 \text{ s}^{-1}$ was measured at pH 7.0 and $50,000 \text{ s}^{-1}$ at pH 10.0. The TOF_{max} value is calculated from the cyclic voltammograms of **11** in the presence of H_2O , with large current densities being observed in the range 1.2–1.5 V at pH 10.0 (FIG. 6a). The appearance of reversible waves ($E_{1/2} \approx 0.6$ and 1.1 V) assigned to the complex are consistent with the molecular species remaining intact under turnover conditions.

Figure 6 | **Voltammetry of $[(\text{tda-}\kappa\text{-N}^3\text{O})(\text{py})_2\text{Ru}^{\text{IV}}(\text{OH})]^+$ (**11**) and $[(\text{mox})\text{Cu}^{\text{II}}]^{2-}$ (**12**) reveals catalytic H_2O oxidation waves. a** | The cyclic voltammogram of **11** at pH 10.0 has two reversible waves as well as a large catalytic wave at high potentials. Density functional theory calculations indicate that the complex operates by using its free carboxylate to relay H^+ to a hydroperoxo ligand. Part **a** adapted with permission from reference [108](#), American Chemical Society. **b** | Voltammetry for **12** at pH 11.5 features a reversible $\text{Cu}^{\text{III/II}}$ wave and a catalytic wave whose onset coincides with the redox couple for coordinated $\text{mox}^{3-/4-}$. Density functional theory calculations suggest, as pictured, the intermediacy of a hydroxo complex of the radical ligand mox^{3-} . mox^{4-} , $N^1, N^{1'}$ -(1,2-phenylene)bis(N^2 -methyloxalamide); py, pyridine; 2,2':6',2''-terpyridine-6,6''-dicarboxylate. Part **b** adapted with permission from reference [141](#), American Chemical Society.

An additional feature of complexes such as **9** and **11** is that the key chemistry occurs solely in the equatorial plane defined by the chelating ligand and Ru–O(H) group; the apical py ligands merely complete the coordination geometry, which is either octahedral or pentagonal bipyramidal depending on the oxidation state. The apical ligand is therefore an ideal site to functionalize the complex without influencing the electronic properties of the Ru centre.^{112,113,114,115,116} For example,

anchoring a derivative of **11** onto conductive solid supports affords electroanodes¹¹⁵ or light-absorbing materials to generate hybrid molecular photonanodes.^{117,118} The Ru-tda²⁻ complexes in this hybrid molecular material still exhibit the solution-phase reactivity of **11**, thus validating the anchoring strategy. Further, the material is the most stable molecular photoanode ever reported for H₂O oxidation. Overall, the key features associated with both the bda²⁻ and tda²⁻ co-ligands include flexibility, adaptability, multidenticity and equatorial coordination. For these reasons we often refer to these privileged systems as FAME ligands.

[H1] First-row molecular WOCs

The ideal solvent in which to conduct H₂O oxidation catalysis is obviously H₂O, but when present in high concentrations H₂O can compete for metal coordination sites and displace co-ligands. This is not a problem for Ru^{II} and Ru^{III} ions because their complexes typically exist in low-spin 4d⁶ and 4d⁵ configurations that are kinetically stable. The only reactive site for polypyridyl-type Ru–OH₂ catalysts is the Ru–OH₂ bond — an ideal scenario because one can rely on the co-ligands remaining firmly attached to Ru and simply being spectator ligands. The substitutional inertness of this type of complexes is exemplified in their Pourbaix diagrams (FIG. 4), which suggest that, aside from H⁺/e⁻ transfers, most of them are perfectly stable within the 0–14 pH range.

In sharp contrast, complexes of Mn, Fe, Co, Ni and Cu are in general substitutionally labile and their stabilities will be highly dependent on their co-ligands and solution pH. For instance, H₂O exchange between the bulk and [M(H₂O)₆]^{3+/2+} is eight orders of magnitude faster for both Fe^{II} and Fe^{III} relative to their Ru^{II} and Ru^{III} counterparts.^{119,120} Further complicating the endeavour of preparing first-row transition metal WOCs is that at low pHs most ligands will undergo decoordination and protonation, as is the case for Fe–polypyridyl complexes.^{121,122} Further, at high pH values the complexes will simply decompose into hydroxides and/or oxides. As the H₂O oxidation reaction proceeds, the solution pH can be drastically reduced because 4H⁺ are released per O₂ molecule evolved. Consequently, when using first-row transition metal WOCs it is crucial to carry out catalysis in buffered solution. An additional problem that arises particularly with first row transition metals is that once the corresponding oxide is formed it can adsorb onto the electrode surface or precipitate from solution as a colloid. These are additional driving forces for the decomposition of the initial complex.¹²³ Interestingly, the deposition of transition metal oxides at electrode surfaces can afford highly active electroanodes for H₂O oxidation. These can be substantially different than those generated at the same pH from the simple metal salts.^{42,124,125,126,127,128,129,130,131,132} For these reasons, following electrocatalysis with the molecular

complexes it is absolutely necessary to check the catalytic activity of the electrode in a clean electrolyte solution. In addition, an excellent way to monitor the stability of the initial molecular catalyst is to measure a non-catalytic Faradaic wave associated with the complex (such a wave will appear at lower potentials than the electrocatalytic process). In this way, the integrity of the initial complex can be easily evaluated during turnover conditions.¹⁴¹

Only a few first-row transition metal complexes are active H₂O oxidation catalysts and abide with the conditions above.^{133,134,135,136,137,138,139,140} One example is [(mox)Cu^{II}]²⁻ (**12**, mox⁴⁻ = *N*¹,*N*^{1'}-(1,2-phenylene)bis(*N*²-methyloxalamide)), in which Cu^{II} is strongly bound to a tetraanionic tetraamidato ligand.^{141,142} The high electron density donated from this ligand enables access to Cu^{III} at a potential of only 0.56 V at pH = 11.5, where the complex is fully stable as evidenced by the reversibility of this Cu^{III/II} wave in cyclic voltammograms (FIG. 6b). At potentials >1.20 V, a large current response is observed that must arise from an electrocatalytic process. In particular, reversible oxidation of the aromatic ring affords a radical cation that readily accepts a OH⁻ ligand (FIG. 6b). Following a WNA step and single electron transfers, one obtains a complex featuring hydrogen bonded H₂O₂, with this moiety then undergoing a series of intramolecular e⁻ transfers to release O₂ and regenerate the initial complex. As mentioned above, one can check that the catalyst remains intact by scanning the potentials at which a reversible wave characteristic of the complex appears. Indeed, the Cu^{III/II} wave is preserved after the electrocatalytic process, reflective of the high robustness of the catalyst under these conditions. An additional piece of evidence supporting this proposed mechanism is the substantial lowering of the overpotential when electron donating groups are installed at the phenylene ring of mox⁴⁻. For instance, the dimethoxy derivative has a ~530 mV lower overpotential relative to that of the parent catalyst **12**. The catalyst **12** is further notable in that it undergoes reversible oxidation not only at its metal centre but also at the organic ligand.

In contrast to well-characterized WOCs like **12**, there are at present a large number of first-row transition metal complexes that are proposed to operate as molecular H₂O oxidation catalysts but whose active species are actually metal oxides. To avoid the unfortunate case of misinterpreting data, we strongly recommend that chemists rigorously check the stability of complexes in solution as well as the activity of a used electrode in a clean electrolyte solution. Neglecting to perform these checks and only measuring the spectroscopic and redox properties of the initial complex can lead to a large waste of time if the initial complexes are not responsible for the H₂O oxidation activity.^{143,144,145,146,147,148,149,150}

[H1] Conclusions and challenges

Molecular WOCs based on Ru have enjoyed a spectacular development over the last decade — arguably a short amount of time to improve TOF values by more than seven orders of magnitude. Additionally, this period has seen us develop a sound description of mechanisms that has helped and will continue to help us achieve improvements in terms of catalytic performance and the identification and avoidance of potential deactivation pathways. In parallel, the lessons learned from studying Ru complexes are at least partially applicable to other transition metal complexes such as those of Ir and first-row transition metals such as Fe, Co and Cu, among others.

Those working on developing improved WOCs still face several challenges. The first of these includes the goal faced by all working in electrocatalysis: to find catalysts that turn over on the nanosecond time scale at potentials as close as possible to the thermodynamic values. Fast catalysts are necessary to improve the efficiencies of H₂O oxidation photoanodes and H₂O-splitting devices because it is the chemical rather than photochemical steps that are typically rate-limiting. In addition, when a charge-separated state is photogenerated we must provide it with a way to immediately participate in the catalytic reaction instead of undergoing degradation. The second challenge is to develop first-row transition metal complexes that are as fast and robust as the best Ru complexes. Although there is no reason why this should be impossible, it is obvious that one needs to pay very careful attention to the idiosyncracies of first-row transition metal complexes and consider their potential lability. By neglecting this, one can overlook the formation of oxides that can end up being the actual catalytically active species. The final challenge is associated with practical electrocatalytic applications, for which molecular species in solution are typically not useful. However, one can obtain high current densities by anchoring highly active catalysts to solid electrodes or semiconductors with large surface coverages. In this way, one can construct technologically useful H₂O-splitting devices that could lead the way towards replacing fossil fuels with solar fuels.

[H1] Acknowledgments

Sustained support from MINECO, FEDER and AGAUR are gratefully acknowledged. Recent grants include CTQ2015-64261-R, CTQ2016-80058-R, CTQ2015-73028-EXP, SEV 2013-0319, ENE2016-82025-REDT, CTQ2016-81923-REDC, and 2017-SGR-1631. The work at Brookhaven National Laboratory (M.Z.E.) was carried out under contract DE-SC0012704 with the U.S. Department of Energy, Office of Science, Office of Basic Energy Sciences, and utilized computational resources at the BNL Center for Functional Nanomaterials (CFN). The CFN is a U.S.

DOE Office of Science Facility at Brookhaven National Laboratory, operating under contract No. DE-SC0012704.

[H1] Author contributions

All authors contributed equally to the preparation of this manuscript.

[H1] Competing interests statement

The authors declare no competing interests.

[H1] Publisher's note

Springer Nature remains neutral with regard to jurisdictional claims in published maps and institutional affiliations.

[H1] How to cite this article

Matheu, R. et al. The development of molecular water oxidation catalysts. *Nat. Rev. Chem.* **3**, xxxxx (2019).

References.

- ¹ Steffen, W. et al. Trajectories of the Earth System in the anthropocene. *Proc. Natl Acad. Sci. USA* **115**, 8252–8259 (2018).
- ² Balmaseda, M. A., Trenberth, K. E. & Källén W. Distinctive climate signals in reanalysis of global ocean heat content. *Geophys. Res. Lett.* **40**, 1754–1759 (2013).
- ³ IPCC *Climate Change 2013: The Physical Science Basis* (Eds Stocker, T. F. et al.) (Cambridge University Press, Cambridge, 2013).
- ⁴ IPCC *Climate Change 2014: Mitigation of Climate Change* (Eds Edenhofer, O. et al.) (Cambridge University Press, Cambridge, 2014).
- ⁵ *Kyoto Protocol to the United Nations Framework Convention On Climate Change*, United Nations Framework Convention on Climate Change (UNFCCC), 1998.
- ⁶ *Adoption of the Paris Agreement. Proposal by the President*, Paris Climate Change Conference – November 2015, COP 21, Paris, France, 2015.
- ⁷ Staher, W. R. The circular economy. *Nature* **531**, 435–438 (2016).
- ⁸ “Annual Energy Outlook 2018 with projections to 2050” by the U.S. Energy Information Administration, **2018**. Available at the web page, “<https://www.eia.gov/outlooks/aeo/>”.
- ⁹ BP Statistical Review of World Energy June 2017.
- ¹⁰ Croce, R. & van Amerongen, H. Natural strategies for photosynthetic light harvesting. *Nat. Chem. Biol.* **10**, 492–501 (2014).
- ¹¹ Nelson, N. & Ben-She, A. The complex architecture of oxygenic photosynthesis. *Nat. Rev. Mol. Cell. Biol.* **5**, 971–982 (2004).
- ¹² McEvoy, J. P. & Brudvig, G. W. Water-splitting chemistry of photosystem II. *Chem. Rev.* **106**, 4455–4483 (2006).
- ¹³ Grätzel, M. Artificial photosynthesis: water cleavage into hydrogen and oxygen by visible light. *Acc. Chem. Res.* **14**, 376–384 (1981)
- ¹⁴ Guan, X. et al. Making of an industry-friendly artificial photosynthesis device. *ACS Energy Lett.* **3**, 2230–2231 (2018).
- ¹⁵ Lewis, N. S. Research opportunities to advance solar energy utilization. *Science* **351**, 353–361 (2016).
- ¹⁶ Nocera, D. G. Solar fuels and solar chemicals industry. *Acc. Chem. Res.* **50**, 616–619 (2017).
- ¹⁷ Roger, I., Shipman, M. A. & Symes, M. D. Earth-abundant catalysts for electrochemical and photoelectrochemical water splitting. *Nat. Rev. Chem.* **1**, 301–313 (2017).
- ¹⁸ Arno de Klerk (2013). “Fischer–Tropsch Process”. Kirk-Othmer Encyclopedia of Chemical Technology. Weinheim: Wiley-VCH.
- ¹⁹ Yu, K. M. K., Curcic, I., Gabriel, J. & Tsang, S. C. E. Recent advances in CO₂ capture and utilization. *ChemSusChem*, **1**, 893–899 (2008).

-
- ²⁰ Oleksandr S. B. et al. What should we make with CO₂ and how can we make it? *Joule* **2**, 825–832 (2018).
- ²¹ www.energy-democracy.net/. Accessed on August 17th, 2018.
- ²² Ferreira, K. N., Iverson, T. M., Maghlaoui, K., Barber, J. & Iwata, S. Architecture of the photosynthetic oxygen-evolving center. *Science* **303**, 1831–1838 (2004).
- ²³ Barber, J. Mn₄Ca cluster of photosynthetic oxygen-evolving center: structure, function and evolution. *Biochemistry* **55**, 5901–5906 (2016).
- ²⁴ Umena, Y., Kawakami, K., Shen, J.-R. & Kamiya, N. Crystal structure of oxygen-evolving photosystem II at a resolution of 1.9 Å. *Nature* **473**, 55–60 (2011)
- ²⁵ Suga, M. et al. Native structure of photosystem II at 1.95 Å resolution viewed by femtosecond X-ray pulses. *Nature* **517**, 99–103 (2015)
- ²⁶ Klaus, A., Haumann, M. & Dau, H. Alternating electron and proton transfer steps in photosynthetic water oxidation. *Proc. Natl Acad. Sci. USA* **109**, 16035–16040 (2012).
- ²⁷ Krewald, V. et al. Metal oxidation states in biological water splitting. *Chem. Sci.* **6**, 1676–1695 (2015).
- ²⁸ Rappaport, F., Guergova-Kuras, M., Nixon, P. J., Diner, B. A. & Lavergne, J. Kinetics and pathways of charge recombination in photosystem II. *Biochemistry* **41**, 8518–8527 (2002).
- ²⁹ Cox, N., Pantazis, D. A., Neese, F. & Lubitz, W. Biological water oxidation. *Acc. Chem. Res.* **46**, 1588–1596 (2013).
- ³⁰ Vogt, L., Vinyard, D. J., Khan, S. & Brudvig, G. W. Oxygen-evolving complex of photosystem II: an analysis of second-shell residues and hydrogen-bonding networks. *Curr. Opin. Chem. Biol.* **25**, 152–158 (2015).
- ³¹ Vass, I. Molecular mechanisms of photodamage in the photosystem II complex. *Biochim. Biophys. Acta* **1817**, 209–217 (2012).
- ³² Hideg, E., Kalai, T., Hideg, K. & Vass, I. Photoinhibition of photosynthesis in vivo results in singlet oxygen production detection via nitroxide-induced fluorescence quenching in broad bean leaves. *Biochemistry* **37**, 11405–11411 (1998).
- ³³ Moyer, B. A. & Meyer, T. J. Proton-coupled electron transfer between [Ru(bpy)₂(py)OH₂]²⁺ and [Ru(bpy)₂(py)O]²⁺. A solvent isotope effect ($k_{\text{H}_2\text{O}}/k_{\text{D}_2\text{O}}$) of 16.1. *J. Am. Chem. Soc.* **100**, 3601–3603 (1978)
- ³⁴ Weinberg, D. R. et al. Proton-coupled electron transfer. *Chem. Rev.* **112**, 4016–4093 (2012).
- ³⁵ Gagliardi, C. J., Vannucci, A. K., Concepcion, J. J., Chen, Z. & Meyer, T. J. The role of proton coupled electron transfer in water oxidation. *Energy Environ. Sci.* **5**, 7704–7717 (2012).
- ³⁶ Savéant, J.-M. Electrochemical approach to proton-coupled electron transfers: recent advances. *Energy Environ. Sci.* **5**, 7718–7731 (2012).
- ³⁷ Glöckner, C. et al. Structural changes of the oxygen-evolving complex in photosystem II during the catalytic cycle. *J. Biol. Chem.* **288**, 22607–22620 (2013).
- ³⁸ Young, I. D. et al. Structure of photosystem II and substrate binding at room temperature. *Nature* **540**, 453–457 (2016).

-
- ³⁹ Suga, M. et al. Light-induced structural changes and the site of O=O bond formation in PSII caught by XFEL. *Nature* **543**, 131–135 (2017).
- ⁴⁰ Cox, N. et al. Electronic structure of the oxygen-evolving complex in photosystem II prior to O–O bond formation. *Science* **345**, 804–808 (2014).
- ⁴¹ Lohmiller, T. et al. The first state in the catalytic cycle of the water-oxidizing enzyme: identification of a water-derived μ -hydroxo bridge. *J. Am. Chem. Soc.* **139**, 14412–14424 (2017).
- ⁴² McCrory, C. C. L. et al. Benchmarking hydrogen evolving reaction and oxygen evolving reaction electrocatalysts for solar water splitting devices. *J. Am. Chem. Soc.* **137**, 4347–4357 (2015).
- ⁴³ Smith, R. D. L. et al. Photochemical route for accessing amorphous metal oxide materials for water oxidation catalysis. *Science*, **340**, 60–63 (2013).
- ⁴⁴ Godwin, I., Rovetta, A., Lyons, M. & Coleman, J. Electrochemical water oxidation: The next five years. *Curr. Opin. Electrochem.* **7**, 31–35 (2018).
- ⁴⁵ Blakemore, J. D., Crabtree, R. H. & Brudvig, G. W. Molecular catalysts for water oxidation. *Chem. Rev.* **115**, 12974–13005 (2015).
- ⁴⁶ Berardi, S. et al. Molecular artificial photosynthesis. *Chem. Soc. Rev.* **43**, 7501–7519 (2014).
- ⁴⁷ Garrido-Barros, P., Gimbert-Suriñach, C., Matheu, R., Sala, X. & Llobet, A. How to make an efficient and robust molecular catalyst for water oxidation. *Chem. Soc. Rev.* **46**, 6088–6098 (2017).
- ⁴⁸ Coehn, A. & Gläser, M. Studien über die Bildung von Metalloxyden. 1. Über das anodische Verhalten von Kobalt- und Nickel-Lösungen. *Zeits. Anorg. Chem.* **33**, 9–24 (1903).
- ⁴⁹ Gersten, S. W., Samuels, G. J. & Meyer, T. J. Catalytic oxidation of water by an oxo-bridged ruthenium dimer. *J. Am. Chem. Soc.* **104**, 4029–4030 (1982).
- ⁵⁰ Elizarova, G. L., Matvienko, L. G., Parmon, V. N. & Zamaraev, K. I. Catalysts of the oxidation of water to molecular oxygen based on binuclear complexes of iron(III) and other compounds of transition metals. *Dokl. Akad. Nauk SSSR*, **249**, 863–866 (1979).
- ⁵¹ Elizarova, G. L., Matvienko, L. G., Lozhkina, N. V., Parmon, V. N. & Zamaraev, K. I. Homogeneous catalysts for dioxygen evolution from water. Water oxidation by trisbipyridylruthenium(III) in the presence of cobalt, iron and copper complexes. *React. Kinet. Catal. Lett.* **16**, 191–194 (1981).
- ⁵² Gilbert, J. A. et al. Structure and redox properties of the water-oxidation catalyst $[(\text{bpy})_2(\text{OH}_2)\text{RuORu}(\text{OH}_2)(\text{bpy})_2]^{4+}$. *J. Am. Chem. Soc.* **107**, 3855–3864 (1985).
- ⁵³ Liu, F. et al. Mechanisms of water oxidation from the blue dimer to Photosystem II. *Inorg. Chem.* **47**, 1727–1752 (2008).
- ⁵⁴ Geselowitz, D. & Meyer, T. J. Water oxidation by $[(\text{bpy})_2(\text{O})\text{Ru}^{\text{V}}\text{ORu}^{\text{V}}(\text{O})(\text{bpy})_2]^{4+}$. An oxygen-labeling study. *Inorg. Chem.* **29**, 3894–3896 (1990).

-
- ⁵⁵ Yamada, H., Siems, W. F., Koike, T. & Hurst, J. K. Mechanisms of water oxidation catalyzed by the *cis,cis*-[(bpy)₂Ru(OH₂)₂O⁴⁺ ion. *J. Am. Chem. Soc.* **126**, 9786–9795 (2004).
- ⁵⁶ Cape, J. L. & Hurst, J. K. Detection and mechanistic relevance of transient ligand radicals formed during [Ru(bpy)₂(OH₂)₂O⁴⁺-catalyzed water oxidation. *J. Am. Chem. Soc.* **130**, 827–829 (2008).
- ⁵⁷ Chronister, C. W., Binstead, R. A., Ni, J. & Meyer, T. J. Mechanism of water oxidation catalyzed by the μ -oxo dimer [(bpy)₂(OH₂)Ru^{III}ORu^{III}(OH₂)(bpy)₂]⁴⁺. *Inorg. Chem.* **36**, 3814–3815 (1997).
- ⁵⁸ Parent, A. R., Crabtree, R. H. & Brudvig, G. W. Comparison of primary oxidants for water-oxidation catalysis. *Chem. Soc. Rev.* **42**, 2247–2252 (2013).
- ⁵⁹ Binstead, R. A., Chronister, C. W., Ni, J., Hartshorn, C. M. & Meyer, T. J. Mechanism of water oxidation by the μ -oxo dimer [(bpy)₂(H₂O)Ru^{III}ORu^{III}(OH₂)(bpy)₂]⁴⁺. *J. Am. Chem. Soc.* **122**, 8464–8473 (2000).
- ⁶⁰ Moonshiram, D. et al. Structure and electronic configurations of the intermediates of water oxidation in blue ruthenium dimer catalysis. *J. Am. Chem. Soc.* **134**, 4625–4636 (2012).
- ⁶¹ Costentin, C., Drouet, S., Robert, M., Savéant, J.-M. Turnover Numbers, Turnover Frequencies, and Overpotential in Molecular Catalysis of Electrochemical Reactions. Cyclic Voltammetry and Preparative-Scale Electrolysis. *J. Am. Chem. Soc.* **134**, 11235–11242 (2012).
- ⁶² Rotzinger, F. P. et al. A molecular water-oxidation catalyst derived from ruthenium diaqua bis(2,2'-bipyridyl-5,5'-dicarboxylic acid). *J. Am. Chem. Soc.* **109**, 6619–6626 (1987).
- ⁶³ Nazeeruddin, M. K., Rotzinger, F. P., Comte, P. & Grätzel, M. Spontaneous oxidation of water to oxygen by the mixed-valence μ -oxo ruthenium dimer L₂(H₂O)Ru–O–Ru(OH)L₂ (L = 2,2'-bipyridyl-5,5'-dicarboxylic acid). *J. Chem. Soc., Chem. Commun.* 872–874 (1988).
- ⁶⁴ Sens, C. et al. A new Ru complex capable of catalytically oxidizing water to molecular dioxygen. *J. Am. Chem. Soc.* **126**, 7798–7799 (2004).
- ⁶⁵ Romain, S., Bozoglian, F., Sala, X. & Llobet, A. Oxygen–oxygen bond formation by the Ru-Hbpp water oxidation catalyst occurs solely via an intramolecular reaction pathway. *J. Am. Chem. Soc.* **131**, 2768–2769 (2009).
- ⁶⁶ Bozoglian, F. et al. The Ru-Hbpp water oxidation catalyst. *J. Am. Chem. Soc.* **131**, 15176–15187 (2009).
- ⁶⁷ Romain, S., Vigara, L. & Llobet, A. Oxygen–oxygen bond formation pathways promoted by Ru complexes. *Acc. Chem. Res.* **42**, 1944–1953 (2009).
- ⁶⁸ Neudeck, S. et al. New powerful and oxidatively rugged dinuclear Ru water oxidation catalyst: control of mechanistic pathways by tailored ligand design. *J. Am. Chem. Soc.* **136**, 24–27 (2014).
- ⁶⁹ Catalano, V. J. et al. Monometallic and dimetallic ruthenium(II)-terpyridine complexes employing the tetradentate ligands dipyridylpyrazolyl, dipyridyloxadiazole, and their dimethyl derivatives. *Inorg. Chem.* **42**, 321–334 (2003).

-
- ⁷⁰ Zong, R. & Thummel, R. P. A new family of Ru complexes for water oxidation. *J. Am. Chem. Soc.* **127**, 12802–12803 (2005).
- ⁷¹ Concepcion, J. J., Jurss, J. W., Templeton, J. L. & Meyer, T. J. One site is enough. Catalytic water oxidation by $[\text{Ru}(\text{tpy})(\text{bpm})(\text{OH}_2)]^{2+}$ and $[\text{Ru}(\text{tpy})(\text{bpz})(\text{OH}_2)]^{2+}$. *J. Am. Chem. Soc.* **130**, 16462–16463 (2008).
- ⁷² Masaoka, S. & Sakai, K. Evidence showing the robustness of a highly active oxygen-evolving mononuclear ruthenium complex with an aqua ligand. *Chem. Lett.* **38**, 182–183 (2009).
- ⁷³ Wasylenko, D.J. et al. Electronic modification of the $[\text{Ru}^{\text{II}}(\text{tpy})(\text{bpy})(\text{OH}_2)]^{2+}$ scaffold: effects on catalytic water oxidation. *J. Am. Chem. Soc.* **132**, 16094–16106 (2010).
- ⁷⁴ Maji, S., López, I., Bozoglian, F., Benet-Buchholz, J. & Llobet, A. Mononuclear ruthenium–water oxidation catalysts: discerning between electronic and hydrogen-bonding effects. *Inorg. Chem.* **52**, 3591–3593 (2013).
- ⁷⁵ Concepcion, J. J. et al. Catalytic water oxidation by single-site ruthenium catalysts. *Inorg. Chem.* **49**, 1277–1279, (2010).
- ⁷⁶ Tong, L. & Thummel, R. P. Mononuclear ruthenium polypyridine complexes that catalyze water oxidation. *Chem. Sci.* **7**, 6591–6603 (2016).
- ⁷⁷ Cytochrome P450: Structure, Mechanism, and Biochemistry (Ed. de Montellano, P. R. O.) (Kluwer Academic/Plenum, New York, ed. 3, 2005).
- ⁷⁸ Rittle, J. & Green M. T. Cytochrome P450 compound I: capture, characterization, and C–H bond activation kinetics. *Science* **330**, 933–937 (2010).
- ⁷⁹ Groves, J. T. Cytochrome P450 enzymes: understanding the biochemical hieroglyphs. F1000Research 2015, 4(F1000 Faculty Rev):178 Last updated: 25 DEC 2016.
- ⁸⁰ López, I., Maji, S., Benet-Buchholz, J. & Llobet, A. Oxo-bridge scenario behind single-site water-oxidation catalysts. *Inorg. Chem.* **54**, 658–666 (2015).
- ⁸¹ Earley, J. E., Smith, P. M., Fealey, T. & Silverton, J. V. Crystal and molecular structure of di- μ -oxo-bis(pentaammineruthenium)bis(ethylenediamine)ruthenium hexachloride. Ethylenediamine analog of "ruthenium red". *Inorg. Chem.* **10**, 1943–1947 (1971).
- ⁸² Tsubonouchi, Y., Lin, S., Parent, A.R., Brudvig, G.W. & Sakai, K. Light-induced water oxidation catalyzed by an oxido-bridged triruthenium complex with a Ru–O–Ru–O–Ru motif. *Chem. Commun.* **52**, 8018–8021 (2016).
- ⁸³ López, I. et al. A self-improved water-oxidation catalyst: is one site really enough? *Angew. Chem. Int. Ed.* **53**, 205–209 (2014).
- ⁸⁴ Radaram, B. et al. Water oxidation by mononuclear ruthenium complexes with TPA-based ligands. *Inorg. Chem.* **50**, 10564–10571 (2011).
- ⁸⁵ Francas, L. et al. Synthesis, structure, and reactivity of new tetranuclear Ru-Hbpp-based water-oxidation Catalysts. *Inorg. Chem.* **50**, 2771–2781 (2011).

-
- ⁸⁶ Sander, A.C., Schober, A., Dechert, S. & Meyer, F. A Pyrazolate-bridged bis(pentadentate) ligand and its dinuclear ruthenium complex. *Eur. J. Inorg. Chem.* **2015**, 4348–4353 (2015).
- ⁸⁷ Garrido-Barros, P. et al. In *Water as an oxygen source for oxidation reactions in Catalytic Oxidations in Organic Synthesis*. (Ed. Muniz, K.) (Georg Thieme Verlag KG, Stuttgart, New York, 2017).
- ⁸⁸ Harriman, A., Pickering, I. J., Thomas, J. M. & Christensen, P. A. Metal oxides as heterogeneous catalysts for oxygen evolution under photochemical conditions. *J. Chem. Soc., Faraday Trans.* **84**, 2795–2806 (1988).
- ⁸⁹ Risch, M. et al. Cobalt-oxo core of a water-oxidizing catalyst film. *J. Am. Chem. Soc.* **131**, 6936–6937 (2009).
- ⁹⁰ Kanan, M. W. et al. Structure and valency of a cobalt–phosphate water oxidation catalyst determined by in situ X-ray spectroscopy. *J. Am. Chem. Soc.*, **132**, 13692–13701 (2010).
- ⁹¹ Elizarova, G. L., Matvienko, L. G. & Parmon, V. N. Oxidation of water by Ru(bpy)³⁺ in the presence of Co(III) and Fe(III) colloidal hydroxides as catalysts. *J. Mol. Catal.* **43**, 171–181 (1987).
- ⁹² Kim, T. V. Elizarova, G. L. & Parmon, V. N. Catalytic oxidation of water to dioxygen by Ru(bpy)³⁺ in the presence of mixed iron and cobalt hydroxides. *React. Kinet. Catal. Lett.* **26**, 57–60 (1984).
- ⁹³ Hull, J. F. et al. Highly active and robust Cp* iridium complexes for catalytic water oxidation. *J. Am. Chem. Soc.* **131**, 8730–8731 (2009).
- ⁹⁴ Zhao, Y. et al. Stable iridium dinuclear heterogeneous catalysts supported on metal oxide substrate for solar water oxidation. *Proc. Natl Acad. Sci. U.S.A.* **115**, 2902–2907 (2018).
- ⁹⁵ Rodriguez, G.M., Gatto, G., Zuccaccia, C. & Machioni, A. Benchmarking water oxidation catalysts based on iridium complexes: clues and doubts on the nature of active species. *ChemSusChem* **10**, 4503–4509 (2017).
- ⁹⁶ Savini, A. et al. Activity and degradation pathways of pentamethyl-cyclopentadienyl-iridium catalysts for water oxidation. *Green Chem.*, **13**, 3360–3374 (2011).
- ⁹⁷ Duan, L., Fischer, A., Xu, Y. & Sun, L. Isolated seven-coordinate Ru(IV) dimer complex with [HOHOH][−] bridging ligand as an intermediate for catalytic water oxidation. *J. Am. Chem. Soc.* **131**, 10397–10399 (2009).
- ⁹⁸ Duan, L. et al. A molecular ruthenium catalyst with water-oxidation activity comparable to that of photosystem II. *Nat. Chem.* **4**, 418–423 (2012).
- ⁹⁹ Matheu, R. et al. The behavior of the Ru–bda water oxidation catalysts at low oxidation states. *Chem. Eur. J.* **24**, 12838–12847 (2018).
- ¹⁰⁰ Nyhlen, J., Duan, L., Aakermark, B., Sun, L. & Privalov, T. Evolution of O₂ in a seven-coordinate Ru^{IV} dimer complex with a [HOHOH][−] bridge: a computational study. *Angew. Chem. Int. Ed.* **49**, 1773–1777 (2010).
- ¹⁰¹ Matheu, R. et al. Hydrogen bonding rescues overpotential in seven-coordinated Ru water oxidation catalysts. *ACS Catal.* **7**, 6525–6532 (2017).
- ¹⁰² Duan, L., Araujo, C. M., Ahlquist, M. S. G. & Sun, L. Highly efficient and robust molecular ruthenium catalysts for water oxidation. *Proc. Natl Acad. Sci. U. S. A.* **109**, 15584–15588 (2012).
- ¹⁰³ Richmond, C. J. et al. *Chem. Eur. J.* **20**, 17282–17286 (2014).

-
- ¹⁰⁴ Wang, L., Duan, L., Wang, Y., Ahlquist, M. S. G. & Sun, L. Highly efficient and robust molecular water oxidation catalysts based on ruthenium complexes. *Chem. Commun.* **50**, 12947–12950 (2014).
- ¹⁰⁵ Xie, Y., Shaffer, D. W. & Concepcion, J. J. O–O radical coupling: from detailed mechanistic understanding to enhanced water oxidation catalysis. *Inorg. Chem.* **57**, 10533–10542 (2018).
- ¹⁰⁵ THIS REFERENCE SHUOULD BE REMOVED
- ¹⁰⁷ Liu, Y. et al. Catalytic water oxidation by ruthenium(II) quaterpyridine (qpy) complexes: evidence for ruthenium(III) qpy-*N,N''*-dioxide as the real catalysts. *Angew. Chem. Int. Ed.* **53**, 14468–14471 (2014).
- ¹⁰⁸ Matheu, R. et al. Intramolecular proton transfer boosts water oxidation catalyzed by a Ru complex. *J. Am. Chem. Soc.* **137**, 10786–10795 (2015).
- ¹⁰⁹ Matheu, R., Neudeck, S., Meyer, F., Sala, X. & Llobet, A. Foot of the wave analysis for mechanistic elucidation and benchmarking applications in molecular water oxidation catalysis. *ChemSusChem* **9**, 3361–3369 (2016).
- ¹¹⁰ Duan, L., Wang, L., Li, F., Li, F. & Sun, L. Highly efficient bioinspired molecular Ru water oxidation catalysts with negative charged backbone ligands. *Acc. Chem. Res.* **48**, 2084–2096 (2015).
- ¹¹¹ Govindarajan, N., Tiwari, A., Ensing, B. & Meijer, E. J. Impact of the ligand flexibility and solvent on the O–O bond formation step in a highly active ruthenium water oxidation catalyst. *Inorg. Chem.* **57**, 13063–13066 (2018).
- ¹¹² Gao, Y. et al. Visible light driven water splitting in a molecular device with unprecedentedly high photocurrent density. *J. Am. Chem. Soc.* **135**, 4219–4222 (2013).
- ¹¹³ Li, F. et al. Highly efficient oxidation of water by a molecular catalyst immobilized on carbon nanotubes. *Angew. Chem. Int. Ed.* **50**, 12276–12279 (2011).
- ¹¹⁴ Sheridan, M.V. et al. Evaluation of chromophore and assembly design in light-driven water splitting with a molecular water oxidation catalyst. *ACS Energy Lett.* **1**, 231–236 (2016).
- ¹¹⁵ Creus, J. et al. A million turnover molecular anode for catalytic water oxidation. *Angew. Chem. Int. Ed.* **55**, 15382–15386 (2016).
- ¹¹⁶ Wang, D. et al. Interfacial deposition of Ru(III) bipyridine-dicarboxylate complexes by ligand substitution for applications in water oxidation catalysis. *J. Am. Chem. Soc.* **140**, 719–726 (2018).
- ¹¹⁷ Matheu, R. et al. Photoelectrochemical behavior of a molecular Ru-based water-oxidation catalyst bound to TiO₂-protected Si photoanodes. *J. Am. Chem. Soc.* **139**, 11345–11348 (2017).
- ¹¹⁸ Grau, S. et al. A hybrid molecular photoanode for efficient light induced water oxidation. *Sustainable Energy Fuels* **2**, 1979–1985 (2018).
- ¹¹⁹ Rapaport, I., Helm, L., Merbach, A. E., Bernhard, P. & Ludi, A. High-pressure NMR kinetics. Part 34. Variable-temperature and variable-pressure NMR kinetic study of solvent exchange on hexaaquaruthenium(3+) and -(2+) and hexakis(acetonitrile)ruthenium(2+). *Inorg. Chem.* **27**, 873–879 (1988).

-
- ¹²⁰ Helm, L. & Merbach, A. E. Inorganic and bioinorganic solvent exchange mechanisms. *Chem. Rev.* **105**, 1923–1960 (2005).
- ¹²¹ Draksharapu, A. et al. Ligand exchange and spin state equilibria of Fe^{II}(N4Py) and related complexes in aqueous media. *Inorg. Chem.* **51**, 900–913 (2012).
- ¹²² Hong, D. et al. Water oxidation catalysis with nonheme iron complexes under acidic and basic conditions: homogeneous or heterogeneous? *Inorg. Chem.* **52**, 9522–9531 (2013).
- ¹²³ Wang, D., Ghirlanda, G. & Allen, J. P. Water oxidation by a nickel–hlycine catalyst. *J. Am. Chem. Soc.* **136**, 10198–10201 (2014).
- ¹²⁴ Kanan, M. W. & Nocera, D. G. In situ formation of an oxygen-evolving catalyst in neutral water containing phosphate and Co²⁺. *Science* **321**, 1072–1075 (2008).
- ¹²⁵ Singh, A., Chang, S. L. Y., Hocking, R. K., Bach, U. & Spiccia, L. Highly active nickel oxide water oxidation catalysts deposited from molecular complexes. *Energy Environ. Sci.* **6**, 579–586 (2013).
- ¹²⁶ Singh, A., Chang, S. L. Y., Hocking, R. K., Bach, U. & Spiccia, L. Anodic deposition of NiO_x water oxidation catalysts from macrocyclic nickel(II) complexes. *Catal. Sci. Technol.* **3**, 1725–1732 (2013).
- ¹²⁷ Brimblecombe, R., Kolling, D. R. J., Bond, A. M., Dismukes, G. C., Swiegers, G. F. & Spiccia, L. Sustained water oxidation by [Mn₄O₄]⁷⁺ core complexes inspired by oxygenic photosynthesis. *Inorg. Chem.* **48**, 7269–7279 (2009).
- ¹²⁸ Hocking, R. K. et al. Water-oxidation catalysis by manganese in a geochemical-like cycle. *Nat. Chem.* **3**, 461–466 (2011).
- ¹²⁹ Kuznetsov, D. A. et al. Ni-based heterogeneous catalyst from a designed molecular precursor for the efficient electrochemical water oxidation. *Chem. Commun.* **52**, 9255–92558 (2016).
- ¹³⁰ Lai, Y.-H., King, T. C., Wright, D. S. & Reisner, E. Scalable one-step assembly of an inexpensive photoelectrode for water oxidation by deposition of a Ti- and Ni-containing molecular precursor on nanostructured WO₃. *Chem. Eur. J.* **19**, 12943–12947(2013).
- ¹³¹ Lai, Y. H., Kato, M., Mersch, D. & Reisner, E. Comparison of photoelectrochemical water oxidation activity of a synthetic photocatalyst system with photosystem II. *Faraday Discuss.* **176**, 199–211 (2014).
- ¹³² Lai, Y.-H., Palm, D. W. & Reisner, E. Multifunctional coatings from scalable single source precursor chemistry in tandem photoelectrochemical water splitting. *Adv. Energy Mater.* **5**, 1501668 (2015).
- ¹³³ Barnett, S. M., Goldberg, K. I. & Mayer, J. M. A soluble copper–bipyridine water-oxidation electrocatalyst. *Nat. Chem.* **4**, 498–502 (2012).
- ¹³⁴ Gerlach, D. L. et al. Studies of the pathways open to copper water oxidation catalysts containing proximal hydroxy groups during basic electrocatalysis. *Inorg. Chem.* **53**, 12689–12698 (2014).
- ¹³⁵ Zhang, T., Wang, C., Liu, S., Wang, J.-L. & Lin, W. A biomimetic copper water oxidation catalyst with low overpotential. *J. Am. Chem. Soc.* **136**, 273–281 (2014).

-
- ¹³⁶ Fisher, K. J., Materna, K. L., Mercado, B. Q., Crabtree, R. H. & Brudvig, G. W. Electrocatalytic water oxidation by a copper(II) complex of an oxidation-resistant ligand. *ACS Catal.* **7**, 3384–3387 (2017).
- ¹³⁷ Wasylenko, D. J., Ganesamoorthy, C., Borau-Garcia, J. & Berlinguette, C. P. Electrochemical evidence for catalytic water oxidation mediated by a high-valent cobalt complex. *Chem. Commun.* **47**, 4249–4251 (2011).
- ¹³⁸ Rigsby, M. L. Cobalt analogs of Ru-based water oxidation catalysts: overcoming thermodynamic instability and kinetic lability to achieve electrocatalytic O₂ evolution. *Chem. Sci.* **3**, 3058–3062 (2012).
- ¹³⁹ Gimbert-Suriñach, C. et al. Structural and spectroscopic characterization of reaction intermediates involved in a dinuclear Co–Hbpp water oxidation catalyst. *J. Am. Chem. Soc.* **138**, 15291–15294 (2016).
- ¹⁴⁰ Han, Y., Wu, Y., Lai, W. & Cao, R. Electrocatalytic water oxidation by a water-soluble nickel porphyrin complex at neutral pH with low overpotential. *Inorg. Chem.* **54**, 5604–5613 (2015).
- ¹⁴¹ Garrido-Barros, P. et al. Redox non-innocent ligand controls water oxidation overpotential in a new family of mononuclear Cu-based efficient catalysts. *J. Am. Chem. Soc.* **137**, 6758–6761 (2015).
- ¹⁴² Funes-Ardoiz, I., Garrido-Barros, P., Llobet, A. & Maseras, F. Single electron transfer steps in water oxidation catalysis. Redefining the mechanistic scenario. *ACS Catal.* **7**, 1712–1719 (2017).
- ¹⁴³ Wang, H.-Y., Mijangos, E., Ott, S. & Thapper, A. Water oxidation catalyzed by a dinuclear cobalt–polypyridine complex. *Angew. Chem. Int. Ed.* **53**, 14499–14502 (2014).
- ¹⁴⁴ Ishizuka, T. et al. Homogeneous photocatalytic water oxidation with a dinuclear Co^{II}–pyridylmethylamine complex. *Inorg. Chem.* **55**, 1154–1164 (2016).
- ¹⁴⁵ Wang, J.-W., Sahoo, P. & Lu, T.-B. Reinvestigation of water oxidation catalyzed by a dinuclear cobalt–polypyridine complex: identification of CoO_x as real heterogeneous catalyst. *ACS Catal.* **6**, 5062–5068 (2016).
- ¹⁴⁶ Zhang, M., Zhang, M.-T., Hou, C., Ke, Z.-F. & Lu, T.-B. Homogeneous electrocatalytic water oxidation at neutral pH by a robust macrocyclic nickel(II) complex. *Angew. Chem. Int. Ed.* **53**, 13042–13048 (2014).
- ¹⁴⁷ Wang, J.-W. Further insight into the electrocatalytic water oxidation by macrocyclic nickel(II) complexes: the influence of steric effect on catalytic activity. *Catal. Sci. Technol.* **7**, 5585–5593 (2017).
- ¹⁴⁸ Najafpour, M. M. & Feizi, H. Water oxidation by Ni(1,4,8,11-tetraazacyclotetradecane)²⁺ in the presence of carbonate: new findings and an alternative mechanism. *Dalton Trans.* **47**, 6519–6527 (2018).
- ¹⁴⁹ Pizzolato, E. et al. Light driven water oxidation by a single site cobalt salophen catalyst. *Chem. Commun.* **49**, 9941–9943 (2013).
- ¹⁵⁰ Najafpour, M. M. & Feizi, H. Water oxidation catalyzed by two cobalt complexes: new challenges and questions. *Catal. Sci. Technol.* **8**, 1840–1848 (2018).